

This is a repository copy of *How Different are the Diamagnetic and Paramagnetic Contributions to Off-Nucleus Shielding in Aromatic and Antiaromatic Rings?*.

White Rose Research Online URL for this paper:

<https://eprints.whiterose.ac.uk/196714/>

Version: Published Version

Article:

Karadakov, Peter Borislavov orcid.org/0000-0002-2673-6804 (2023) How Different are the Diamagnetic and Paramagnetic Contributions to Off-Nucleus Shielding in Aromatic and Antiaromatic Rings? *ChemPhysChem*. e202300038. ISSN 1439-4235

<https://doi.org/10.1002/cphc.202300038>

Reuse

This article is distributed under the terms of the Creative Commons Attribution (CC BY) licence. This licence allows you to distribute, remix, tweak, and build upon the work, even commercially, as long as you credit the authors for the original work. More information and the full terms of the licence here:

<https://creativecommons.org/licenses/>

Takedown

If you consider content in White Rose Research Online to be in breach of UK law, please notify us by emailing eprints@whiterose.ac.uk including the URL of the record and the reason for the withdrawal request.

Excellence in Chemistry Research



Announcing our new flagship journal

- Gold Open Access
- Publishing charges waived
- Preprints welcome
- Edited by active scientists

Meet the Editors of *ChemistryEurope*



Luisa De Cola
Università degli Studi
di Milano Statale, Italy



Ive Hermans
University of
Wisconsin-Madison, USA



Ken Tanaka
Tokyo Institute of
Technology, Japan

How Different are the Diamagnetic and Paramagnetic Contributions to Off-Nucleus Shielding in Aromatic and Antiaromatic Rings?

Peter B. Karadakov*^[a]

The spatial variations in the diamagnetic and paramagnetic contributions to the off-nucleus isotropic shielding, $\sigma_{\text{iso}}(\mathbf{r}) = \sigma_{\text{iso}}^{\text{d}}(\mathbf{r}) + \sigma_{\text{iso}}^{\text{p}}(\mathbf{r})$, and to the zz component of the off-nucleus shielding tensor, $\sigma_{\text{zz}}(\mathbf{r}) = \sigma_{\text{zz}}^{\text{d}}(\mathbf{r}) + \sigma_{\text{zz}}^{\text{p}}(\mathbf{r})$, around benzene (C_6H_6) and cyclobutadiene (C_4H_4) are investigated using complete-active-space self-consistent field wavefunctions. Despite the substantial differences between $\sigma_{\text{iso}}(\mathbf{r})$ and $\sigma_{\text{zz}}(\mathbf{r})$ around the aromatic C_6H_6 and the antiaromatic C_4H_4 , the diamagnetic and paramagnetic contributions to these quantities, $\sigma_{\text{iso}}^{\text{d}}(\mathbf{r})$ and $\sigma_{\text{zz}}^{\text{d}}(\mathbf{r})$, and $\sigma_{\text{iso}}^{\text{p}}(\mathbf{r})$ and $\sigma_{\text{zz}}^{\text{p}}(\mathbf{r})$, are found to behave similarly in the two molecules, shielding and deshield-

ing, respectively, each ring and its surroundings. The different signs of the most popular aromaticity criterion, the nucleus-independent chemical shift (NICS), in C_6H_6 and C_4H_4 are shown to follow from a change in the balance between the respective diamagnetic and paramagnetic contributions. Thus, the different NICS values for antiaromatic and aromatic molecules cannot be attributed to differences in the ease of access to excited states only; differences in the electron density, which determines the overall bonding picture, also play an important role.

Introduction

The nucleus-independent chemical shift (NICS) suggested by Schleyer and co-workers^[1] is currently by far the most popular aromaticity criterion; a detailed overview of the phenomena of aromaticity and antiaromaticity and the ways in which these can be assessed can be found in a recent monograph.^[2] Initially, the NICS was defined as the off-nucleus isotropic shielding evaluated at the centre of an aromatic or antiaromatic ring and taken with inversed sign, $-\sigma_{\text{iso}}(\mathbf{r}=\text{ring centre})$ [this is now known as NICS(0)]; at position \mathbf{r} , $\sigma_{\text{iso}}(\mathbf{r})$ is given by the average of the diagonal elements of the off-nucleus shielding tensor $\sigma(\mathbf{r})$, $\sigma_{\text{iso}}(\mathbf{r}) = \frac{1}{3}[\sigma_{\text{xx}}(\mathbf{r}) + \sigma_{\text{yy}}(\mathbf{r}) + \sigma_{\text{zz}}(\mathbf{r})]$. The rationale behind this definition was to mimic the chemical shifts of protons residing within the interiors of aromatic or antiaromatic rings – these shifts have been observed to be affected by aromatic or antiaromatic environments much more than are the shifts of exterior protons. Subsequent attempts to improve the accuracy of relative aromaticity assessments led to the formulation of further NICS indices including NICS(1) = $-\sigma_{\text{iso}}(\mathbf{r}=1 \text{ \AA above ring centre})$,^[3–4] NICS(0)_{zz} = $-\sigma_{\text{zz}}(\mathbf{r}=\text{ring centre})$ ^[5–6] and NICS(1)_{zz} = $-\sigma_{\text{zz}}(\mathbf{r}=1 \text{ \AA above ring centre})$ ^[7] (the z axis is assumed to be perpendicular to the ring), and various “dissected” NICS indices

(for details, see e.g. Refs. [4,7]). Despite their widely recognised utility, single-point NICS have been criticised for the arbitrariness in the choice of locations at which these quantities are calculated (NICS can exhibit strong positional dependence and, in certain situations, standard choices can be inappropriate^[8–9]), and there have been claims that a single number might not be sufficient to characterize all aspects of aromatic behaviour, as is illustrated by the observation that different ring current maps can produce nearly indistinguishable single-point NICS values.^[10–11] These criticisms can be addressed by calculating, instead of a single-point NICS, off-nucleus shielding data over sufficiently dense two- or three-dimensional grids of points and analysing off-nucleus shielding as a function of position in space by means of contour plots and isosurfaces (see, for example, refs. [12–14]). Within molecular space, $\sigma_{\text{iso}}(\mathbf{r})$ has been observed to include regions of increased positive $\sigma_{\text{iso}}(\mathbf{r})$ values that can be associated with more intensive electron activity – as a rule, chemical bonds turn out to be well-shielded – in an aromatic ring this leads to the establishment of a doughnut-shaped shielded region encompassing the whole ring which suggests strong bonding interactions and aromatic character.^[12–13] Alternatively, regions of negative $\sigma_{\text{iso}}(\mathbf{r})$ values spreading out from the centres of antiaromatic rings are indicative of antiaromaticity and weakened bonding.^[13,15] It has been suggested that the rather different off-nucleus shielding behaviours observed in aromatic and antiaromatic systems can be viewed as aromatic and antiaromatic “fingerprints” that can be used to identify the aromatic or antiaromatic character not only of the ground but also of the low-lying electronic excited states of a cyclic conjugated system.^[13]

Similarly to a nuclear shielding tensor, the off-nucleus shielding tensor $\sigma(\mathbf{r})$ can be separated into diamagnetic and paramagnetic contributions, $\sigma(\mathbf{r}) = \sigma^{\text{d}}(\mathbf{r}) + \sigma^{\text{p}}(\mathbf{r})$. If calculated

[a] Prof. Dr. P. B. Karadakov
Department of Chemistry
University of York
Heslington, York YO10 5DD, UK
E-mail: peter.karadakov@york.ac.uk

Supporting information for this article is available on the WWW under <https://doi.org/10.1002/cphc.202300038>

© 2023 The Authors. ChemPhysChem published by Wiley-VCH GmbH. This is an open access article under the terms of the Creative Commons Attribution License, which permits use, distribution and reproduction in any medium, provided the original work is properly cited.

with gauge-including atomic orbitals (GIAOs), $\sigma^{\text{GIAO}}(\mathbf{r})$ is gauge-invariant; $\sigma(\mathbf{r})$ calculated with standard field-independent AOs becomes gauge-invariant in the basis set limit. In both cases, the diamagnetic and paramagnetic contributions to the off-nucleus shielding tensor remain dependent on the choice of the gauge origin. By analogy with the approach used to establish a relationship between nuclear shielding and spin-rotation tensors,^[16–18] the paramagnetic contribution to the off-nucleus shielding tensor can be defined as

$$\sigma^{\text{p}}(\mathbf{r}) = \sigma^{\text{GIAO}}(\mathbf{r}) - \sigma^{\text{d}}(\mathbf{r}, \mathbf{R}_g = \mathbf{r}) \quad (1)$$

where $\sigma^{\text{d}}(\mathbf{r}, \mathbf{R}_g = \mathbf{r})$ is the diamagnetic contribution to the off-nucleus shielding at position \mathbf{r} , for a gauge origin \mathbf{R}_g at the same position, calculated as an expectation value over the ground state wavefunction with standard field-independent AOs. $\sigma^{\text{p}}(\mathbf{r})$ depends on the extent to which the ground state wavefunction can be perturbed by an external magnetic field; to first order this perturbation can be expressed as the well-known sum of terms inversely proportional to the differences $E_0 - E_k$ between the ground and excited state energies (E_0 and E_k , respectively).^[16]

In order to gain better understanding of the reasons behind the rather different NICS values and off-nucleus shielding behaviours observed in aromatic and antiaromatic systems, as well as further insights into the much discussed but still somewhat “fuzzy” concepts of aromaticity and antiaromaticity, in this paper we compare and analyse the variations of the diamagnetic and paramagnetic contributions to the off-nucleus isotropic shielding $\sigma_{\text{iso}}(\mathbf{r})$ and to the zz component of the off-nucleus shielding tensor $\sigma_{zz}(\mathbf{r})$ within the spaces surrounding the classical examples of aromatic and antiaromatic molecules, benzene and square cyclobutadiene. The aromaticity of benzene and the antiaromaticity of cyclobutadiene are thought to arise mainly from their π electron systems; in addition, the electronic ground state of square cyclobutadiene, an open-shell singlet, requires at least a two-determinant wavefunction. Therefore, the data required to depict the variations of the diamagnetic and paramagnetic contributions to $\sigma_{\text{iso}}(\mathbf{r})$ and $\sigma_{zz}(\mathbf{r})$ in the two molecules is obtained through shielding calculations utilising complete active space self-consistent field (CASSCF) wavefunctions, with “6 electrons in 6 orbitals” and “4 electrons in 4 orbitals”, for C_6H_6 and C_4H_4 , respectively, which account for the nondynamic π electron correlation effects.

Results and Discussion

As the current CASSCF and CASSCF-GIAO calculations were carried out at the same geometries and in the same 6-311++G(2d,2p) basis set which were used in previous calculations on the electronic ground states of benzene and cyclobutadiene,^[13,19] all CASSCF energies and CASSCF-GIAO shielding data turned out to be exactly the same as those reported earlier.

The carbon and proton isotropic shieldings, the zz components of the carbon and proton shielding tensors, the NICS(0), NICS(0)_{zz}, NICS(1) and NICS(1)_{zz} values, and the diamagnetic and paramagnetic contributions to these quantities for the electronic ground states of benzene and square cyclobutadiene are shown in Table 1. The “combined” values (the sums of the diamagnetic and paramagnetic contributions) of all shielding quantities included in Table 1 were discussed in detail in Ref. [19]. All of the NICS indices distinguish clearly between the aromatic benzene (negative NICS values) and the very antiaromatic square cyclobutadiene (large positive NICS values); the lower $\sigma_{\text{iso}}(\text{H})$ and $\sigma_{zz}(\text{H})$ values for benzene and the higher values of these quantities for square cyclobutadiene are also consistent with aromatic and antiaromatic behaviours, respectively. The diamagnetic contributions to $\sigma_{\text{iso}}(\text{C})$, $\sigma_{zz}(\text{C})$, $\sigma_{\text{iso}}(\text{H})$ and $\sigma_{zz}(\text{H})$ in both of C_6H_6 and C_4H_4 are positive and have a shielding effect; the negative diamagnetic contributions to NICS(0), NICS(0)_{zz}, NICS(1) and NICS(1)_{zz} for both molecules also have a shielding effect (remember that the NICS is a shielding with an inverted sign). The paramagnetic contributions to all of these quantities have a deshielding effect. Thus, the paramagnetic and diamagnetic contributions to all shielding quantities included in Table 1 retain their signs between the aromatic C_6H_6 and the antiaromatic C_4H_4 . However, the balance between these contributions changes between the two molecules – this leads to pronounced differences between the “combined” values and even to opposite NICS signs.

The diamagnetic contributions to $\sigma_{\text{iso}}(\text{C})$, NICS(0) and NICS(1) reported in Table 1 can be approximated using a simple expression for the diamagnetic contribution to the isotropic shielding of nucleus K in a molecule introduced by Flygare and Goodisman:^[20]

$$\sigma_{\text{iso}}^{\text{d}}(K) \approx \sigma_{\text{iso}}^{\text{d}}(\text{free atom } K) + \frac{10^6 e^2}{12\pi\epsilon_0 m c^2} \sum_{J \neq K} \frac{Z_J}{R_{JK}} \quad (2)$$

Table 1. Carbon and proton shieldings, NICS(0), NICS(0)_{zz}, NICS(1) and NICS(1)_{zz} values, and the diamagnetic (“d”) and paramagnetic (“p”) contributions to these quantities for the electronic ground states of benzene and square cyclobutadiene (in ppm). CASSCF and CASSCF-GIAO calculations in the 6-311++G(2d,2p) basis set.

Molecule	$\sigma_{\text{iso}}(\text{C})$	$\sigma_{zz}(\text{C})$	$\sigma_{\text{iso}}(\text{H})$	$\sigma_{zz}(\text{H})$	NICS(0)	NICS _{zz} (0)	NICS(1)	NICS _{zz} (1)
C_6H_6	73.52	186.58	24.90	21.07	−8.17	−12.21	−9.53	−27.83
d	434.51	506.73	185.65	254.24	−262.21	−362.79	−217.74	−222.12
p	−360.99	−320.15	−160.75	−233.17	254.04	350.58	208.21	194.29
C_4H_4	68.24	124.97	27.60	30.34	36.41	145.91	28.23	88.14
d	386.77	437.06	146.71	197.18	−230.51	−305.70	−172.91	−148.15
p	−318.53	−312.09	−119.11	−166.84	266.92	451.61	201.14	236.29

where $\sigma_{\text{iso}}^{\text{d}}$ (free atom K) stands for the diamagnetic contribution to the isotropic shielding of the free atom K , Z_j is the atomic number of nucleus J , R_{JK} is the distance between nuclei J and K , and e , ϵ_0 , m and c are the electron charge, vacuum electric permittivity, electron mass and speed of light, respectively (in SI units). $\sigma_{\text{iso}}^{\text{d}}$ (free atom K) values for $2 \leq Z_K \leq 86$ calculated using numerical Hartree-Fock wavefunctions have been reported by Malli and Froese,^[21] their value for $Z_K=6$ is 260.74 ppm. $\sigma_{\text{iso}}^{\text{d}}$ (free atom K) = 0 at off-nucleus positions such as those used in the definitions of NICS(0) and NICS(1). Eq. (2) produces $\sigma_{\text{iso}}^{\text{d}}$ (C) values of 433.59 and 385.96 ppm, NICS^d(0) values of -264.89 and -238.22 ppm and NICS^d(1) values of -217.96 and -173.73 ppm, for C₆H₆ and C₄H₄, respectively. The agreement between these numbers and the corresponding CASSCF/6-311 + G(2d,2p) results in Table 1 is very good; the only larger deviation is observed for NICS^d(0) in C₄H₄ which is an indication that accounting for the singlet diradical character of this molecule ensures more accurate $\sigma_{\text{iso}}^{\text{d}}(\mathbf{r}, \mathbf{R}_g = \mathbf{r})$ values at and near the centre of the ring. The errors in the approximate $\sigma_{\text{iso}}^{\text{d}}(\mathbf{r}, \mathbf{R}_g = \mathbf{r})$ values obtained using Eq. (2) become much larger closer to atomic positions and along chemical bonds. The level of agreement between the approximate diamagnetic contributions to $\sigma_{\text{iso}}(\text{C})$, NICS(0) and NICS(1) obtained using Eq. (2) and the data reported in Table 1 suggests that the main reason for the larger magnitudes of the diamagnetic contributions to these quantities in benzene, in comparison to their counterparts in square cyclobutadiene, is the increase in the number of atoms.

As an antiaromatic molecule, square cyclobutadiene has lower vertical excitation energies than benzene, for example, the $S_1 \leftarrow S_0$ and $S_2 \leftarrow S_0$ vertical excitation energies for D_{4h} C₄H₄ calculated with state-optimised CASSCF(4,4)/6-311 + G(2d,2p) wavefunctions turned out to be 2.24 eV and 3.48 eV, respectively,^[19] whereas the corresponding vertical excitation energies for D_{6h} C₆H₆ calculated with state-optimised CASSCF(6,6)/6-311 + G(2d,2p) wavefunctions were obtained as 4.96 eV and 7.82 eV.^[13,19] These vertical excitation energies suggest that the π space CASSCF(4,4) wavefunction for square cyclobutadiene should be easier to perturb by an external magnetic field than is the π space CASSCF(6,6) wavefunction for benzene; as a consequence, the paramagnetic contributions to the shielding quantities for C₄H₄ in Table 1 can be expected to be larger in magnitude than those for C₆H₆. In fact, this expectation is confirmed by the paramagnetic contributions to only three of the eight quantities reported in Table 1, NICS(0), NICS_{zz}(0) and NICS_{zz}(1). On the other hand, the magnitudes of the diamagnetic contributions to all shielding quantities in Table 1 decrease on passing from C₆H₆ to C₄H₄; except for $\sigma_{\text{iso}}(\text{H})$, $\sigma_{zz}(\text{H})$ and NICS(0)_{zz}, the associated changes are more pronounced than the parallel changes in the respective paramagnetic contributions. Thus, it is not possible to attribute the significant differences in the values of the popular aromaticity criteria NICS(0), NICS(0)_{zz}, NICS(1) and NICS(1)_{zz} between the aromatic C₆H₆ and the antiaromatic C₄H₄ to changes in the paramagnetic contribution to the shielding tensor only; the data in Table 1 demonstrates that changes in the diamagnetic contribution are very much equally important.}}

Values for the shielding quantities for the electronic ground state of benzene included in Table 1 and for the respective diamagnetic and paramagnetic contributions can also be calculated with a number of closed-shell approaches. HF-GIAO (Hartree-Fock with GIAOs) and MP2-GIAO (second order Møller-Plesset perturbation theory with GIAOs) results for $\sigma_{\text{iso}}(\text{C})$, $\sigma_{zz}(\text{C})$, $\sigma_{\text{iso}}(\text{H})$, $\sigma_{zz}(\text{H})$, NICS(0), NICS(0)_{zz}, NICS(1) and NICS(1)_{zz} in the 6-311 + G(2d,2p) basis set have been reported previously.^[19] The values of NICS(0), NICS(0)_{zz}, NICS(1) and NICS(1)_{zz} for benzene, and the diamagnetic and paramagnetic contributions to these quantities reported in Table 1 can be compared to the scans of NICS(r) and its in-plane (xx and yy) and out-of-plane (zz) components, and the respective diamagnetic and paramagnetic contributions along a line normal to the ring centre in benzene calculated at the B3LYP-GIAO/6-311 + G(d,p) level.^[22] The calculations in Ref. [22] assume a single gauge origin at the centre of mass and use the definitions of the diamagnetic and paramagnetic components of the shielding tensor from Ditchfield's approach.^[23] The NICS(r) and NICS(r)_{zz} values at scan heights of $r=0$ Å and $r=1$ Å from Ref. [22] are close to the values reported in Table 1 but the respective diamagnetic and paramagnetic contributions show large deviations, for example, according to the plots in Ref. [22] NICS^d(0) \approx -33 ppm, NICS^p(0) \approx 25 ppm, NICS^d(1) \approx -16 ppm and NICS^p(1) \approx 5 ppm. Clearly, the NICS^d(0) and NICS^d(1) values obtained with Ditchfield's approach are very different from the rather accurate estimates provided by Eq. (2) and they are unlikely to approach these estimates in the basis set limit. This observation suggests that the conclusions made on the basis of the scans of diamagnetic and paramagnetic contributions to NICS(r) and NICS(r)_{zz} in Ref. [22] would need to be revised if these contributions were to be re-calculated using the more consistent approach adopted in the current work.

The relatively close values of the diamagnetic and paramagnetic contributions to the CASSCF NICS(1) and NICS(1)_{zz} values for benzene in Tables 1 are in agreement with the results of a correlation analysis between NICS criteria and integrated bond current strengths according to which the NICS_{iso}(1) and NICS_{zz}(1) values of benzene and a large set of five- and six-membered heterocycles have well-balanced contributions from the diatropic and paratropic components of the total current density.^[24]}

The positional dependencies of all quantities involved in the expressions $\sigma_{\text{iso}}^{\text{p}}(\mathbf{r}) = \sigma_{\text{iso}}^{\text{GIAO}}(\mathbf{r}) - \sigma_{\text{iso}}^{\text{d}}(\mathbf{r}, \mathbf{R}_g = \mathbf{r})$ and $\sigma_{zz}^{\text{p}}(\mathbf{r}) = \sigma_{zz}^{\text{GIAO}}(\mathbf{r}) - \sigma_{zz}^{\text{d}}(\mathbf{r}, \mathbf{R}_g = \mathbf{r})$ are illustrated by the contour plots in Figures 1–4. To accommodate the wide ranges of variation of the six shielding quantities and still show sufficient detail, the contour levels have been selected individually for each plot, but the colouring in shades of blue for shielded areas and shades of red of deshielded areas is consistent between contour plots.

The isotropic shielding contour plots in Figures 1 and 2 are based on the same data as the analogous contour plots shown in Refs. [12–14]; the changes in appearance (namely, the less visually emphasised shielded and deshielded regions) are due to the use of a different colouring scheme. The $\sigma_{\text{iso}}^{\text{GIAO}}(\mathbf{r})$ contour plots for benzene in Figures 1 and 3 correspond to two cuts

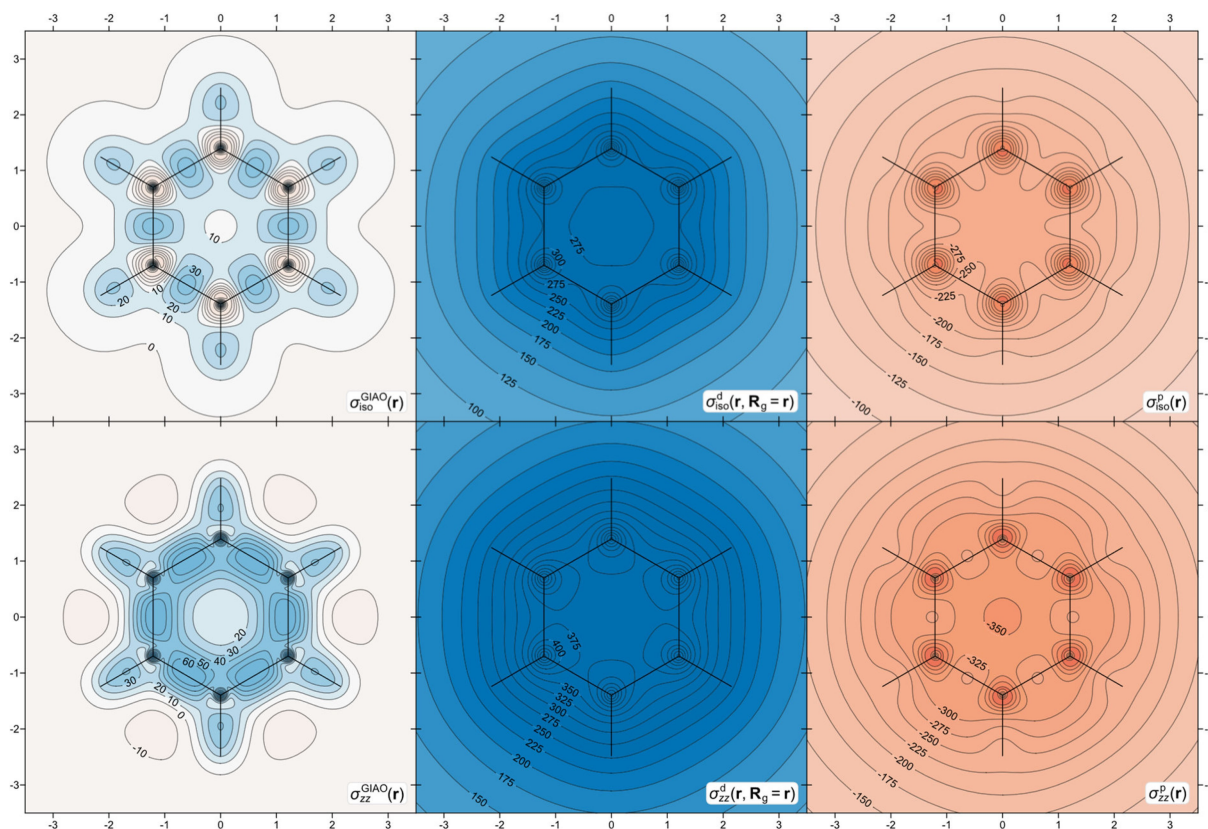


Figure 1. $\sigma_{\text{iso}}^{\text{GIAO}}(\mathbf{r})$, $\sigma_{\text{iso}}^{\text{d}}(\mathbf{r}, \mathbf{R}_{\text{g}} = \mathbf{r})$, $\sigma_{\text{iso}}^{\text{p}}(\mathbf{r})$, $\sigma_{\text{zz}}^{\text{GIAO}}(\mathbf{r})$, $\sigma_{\text{zz}}^{\text{d}}(\mathbf{r}, \mathbf{R}_{\text{g}} = \mathbf{r})$ and $\sigma_{\text{zz}}^{\text{p}}(\mathbf{r})$ contour plots in the molecular (horizontal) plane for the electronic ground state of benzene from “6 in 6” CASSCF and CASSCF-GIAO calculations in the 6-311++G(2d,2p) basis set. Contour levels in ppm, axes in Å.

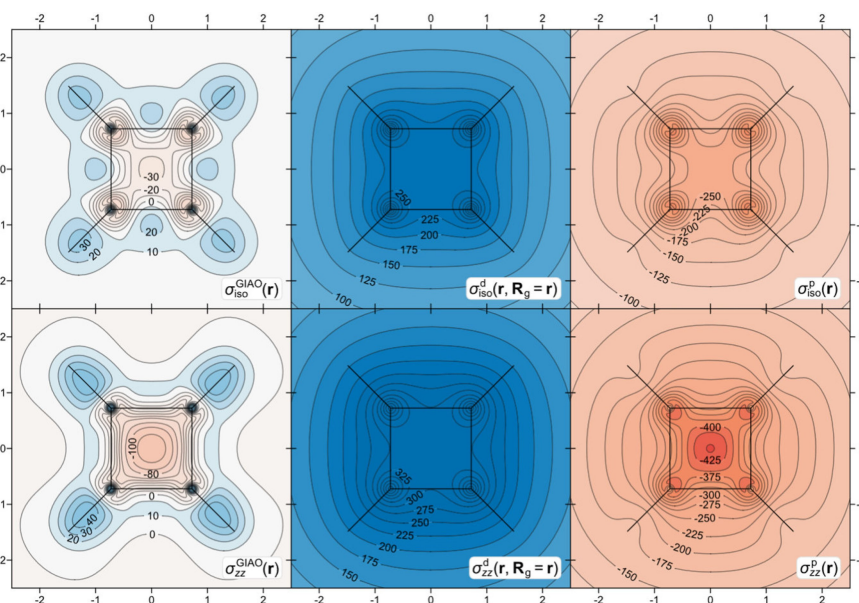


Figure 2. $\sigma_{\text{iso}}^{\text{GIAO}}(\mathbf{r})$, $\sigma_{\text{iso}}^{\text{d}}(\mathbf{r}, \mathbf{R}_{\text{g}} = \mathbf{r})$, $\sigma_{\text{iso}}^{\text{p}}(\mathbf{r})$, $\sigma_{\text{zz}}^{\text{GIAO}}(\mathbf{r})$, $\sigma_{\text{zz}}^{\text{d}}(\mathbf{r}, \mathbf{R}_{\text{g}} = \mathbf{r})$ and $\sigma_{\text{zz}}^{\text{p}}(\mathbf{r})$ contour plots in the molecular (horizontal) plane for the electronic ground state of square cyclobutadiene from “4 in 4” CASSCF and CASSCF-GIAO calculations in the 6-311++G(2d,2p) basis set. Contour levels in ppm, axes in Å.

through the thick shielded “doughnut” enclosing the carbon ring^[12–14] which can be associated with strong bonding interactions and aromatic stability. The $\sigma_{\text{iso}}^{\text{GIAO}}(\mathbf{r})$ contour plots for

square C_4H_4 in Figures 2 and 4 illustrate the presence of a central deshielded region^[12–14] which eliminates most of the shielding over C–C bonds, weakens these bonds and displaces

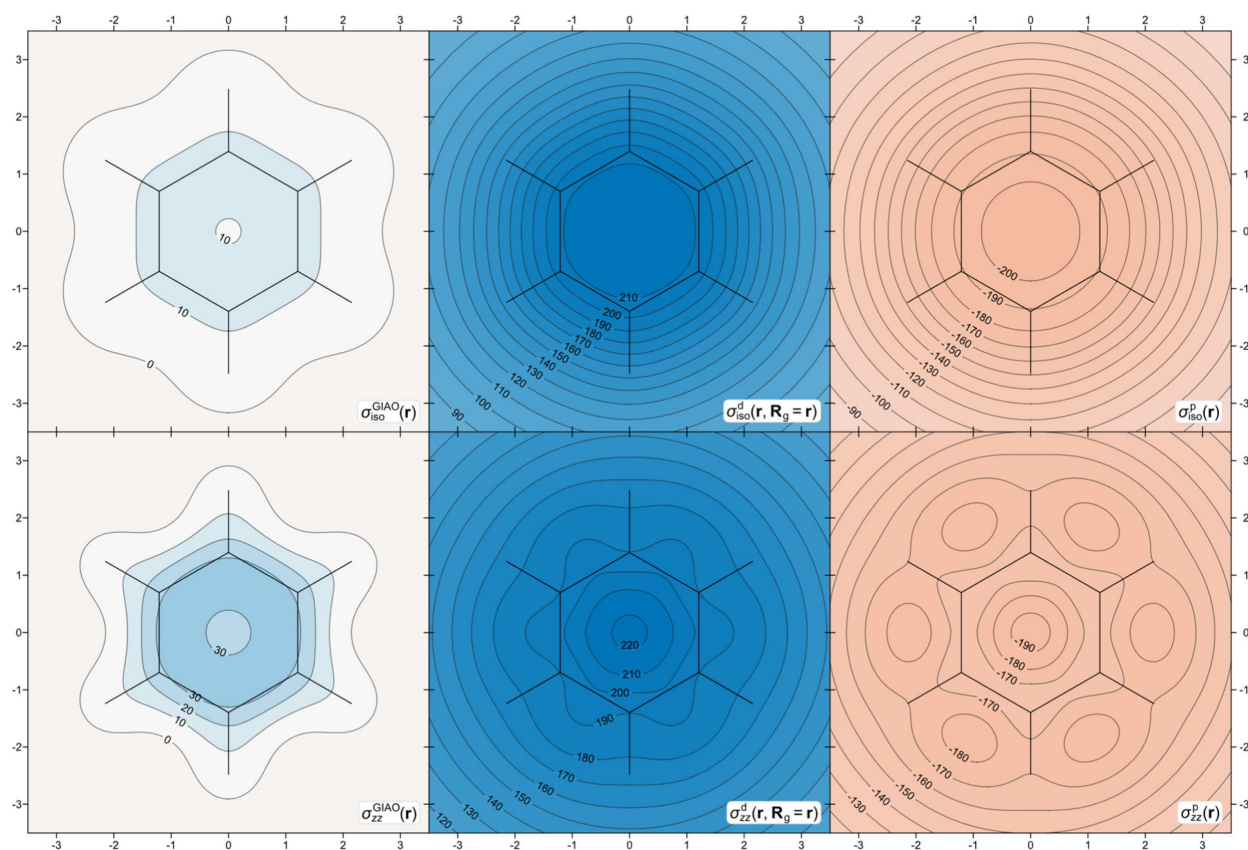


Figure 3. $\sigma_{\text{iso}}^{\text{GIAO}}(\mathbf{r})$, $\sigma_{\text{iso}}^{\text{d}}(\mathbf{r}, \mathbf{R}_g = \mathbf{r})$, $\sigma_{\text{iso}}^{\text{p}}(\mathbf{r})$, $\sigma_{\text{zz}}^{\text{GIAO}}(\mathbf{r})$, $\sigma_{\text{zz}}^{\text{d}}(\mathbf{r}, \mathbf{R}_g = \mathbf{r})$ and $\sigma_{\text{zz}}^{\text{p}}(\mathbf{r})$ contour plots in plane parallel to and 1 Å above the molecular plane for the electronic ground state of benzene from “6 in 6” CASSCF and CASSCF-GIAO calculations in the 6-311++G(2d,2p) basis set. Contour levels in ppm, axes in Å.

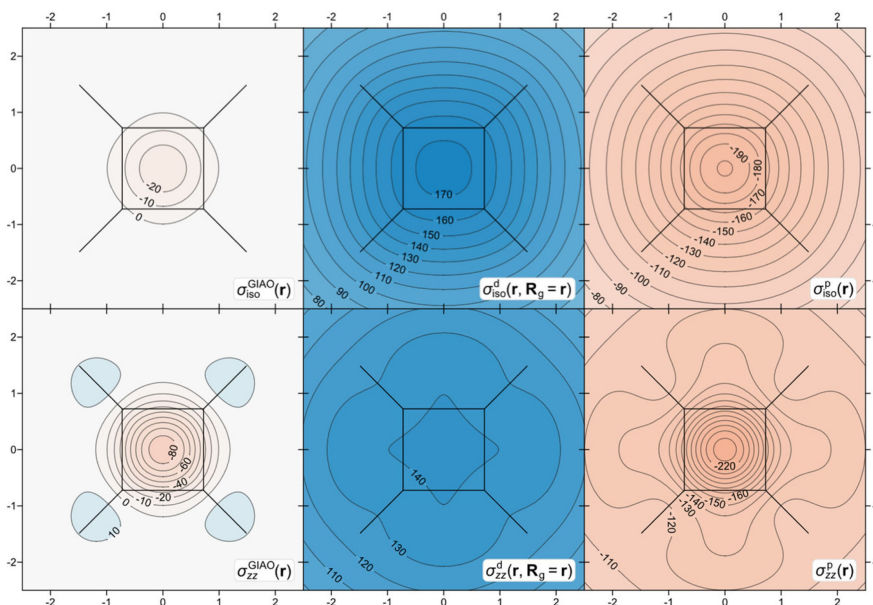


Figure 4. $\sigma_{\text{iso}}^{\text{GIAO}}(\mathbf{r})$, $\sigma_{\text{iso}}^{\text{d}}(\mathbf{r}, \mathbf{R}_g = \mathbf{r})$, $\sigma_{\text{iso}}^{\text{p}}(\mathbf{r})$, $\sigma_{\text{zz}}^{\text{GIAO}}(\mathbf{r})$, $\sigma_{\text{zz}}^{\text{d}}(\mathbf{r}, \mathbf{R}_g = \mathbf{r})$ and $\sigma_{\text{zz}}^{\text{p}}(\mathbf{r})$ contour plots in plane parallel to and 1 Å above the molecular plane for the electronic ground state of square cyclobutadiene from “4 in 4” CASSCF and CASSCF-GIAO calculations in the 6-311++G(2d,2p) basis set. Contour levels in ppm, axes in Å.

the remaining shielding towards the exterior of the ring. Computational experience has shown that isotropic shielding distributions similar to those in the electronic ground states of benzene and square cyclobutadiene are observed in other electronic states and other conjugated rings; these types of distribution can be used for the unambiguous and semi-quantitative classification of the local degree of aromaticity not only of the ground but also of low-lying excited $\pi\pi^*$ electronic states of cyclic conjugated systems and provide a convenient tool for studying excited state aromaticity reversals.^[13,15,19,25–29]

As shown in Figures 1–4, in both of C_6H_6 and C_4H_4 $\sigma_{iso}^d(\mathbf{r}, \mathbf{R}_g = \mathbf{r})$ is positive throughout and has a shielding effect, whereas $\sigma_{iso}^p(\mathbf{r})$ is negative throughout and has a deshielding effect. Overall, the spatial variations of the diamagnetic contribution to the off-nucleus isotropic shielding in C_6H_6 and C_4H_4 are qualitatively similar, and so are the spatial variations of the respective paramagnetic contribution. Whereas the similarity between the spatial variations of $\sigma_{iso}^d(\mathbf{r}, \mathbf{R}_g = \mathbf{r})$ in C_6H_6 and C_4H_4 could have been expected because of the observation that, with certain restrictions (see above), Eq. (2) works reasonably well for both molecules, the similarity between the spatial variations of $\sigma_{iso}^p(\mathbf{r})$ is somewhat unexpected, given the substantial differences between the properties of aromatic and antiaromatic molecules.

Comparing the six- and four-membered rings, $\sigma_{iso}^d(\mathbf{r}, \mathbf{R}_g = \mathbf{r})$ is more positive within the interior of the six-membered ring, and $\sigma_{iso}^p(\mathbf{r})$ is more negative within the interior of the four-membered ring. This change in the balance between $\sigma_{iso}^d(\mathbf{r}, \mathbf{R}_g = \mathbf{r})$ and $\sigma_{iso}^p(\mathbf{r})$ is behind the rather different spatial variations of $\sigma_{iso}^{GIAO}(\mathbf{r})$ in benzene and square cyclobutadiene. In both molecules, $\sigma_{iso}^{GIAO}(\mathbf{r})$ quickly approaches zero with the increase of the distance from the ring centre; $\sigma_{iso}^d(\mathbf{r}, \mathbf{R}_g = \mathbf{r})$ and $\sigma_{iso}^p(\mathbf{r})$ also decrease, but much more slowly because, as a consequence of Eq. (2), outside the ring each of these quantities becomes inversely proportional to the distance from the ring centre.

The $\sigma_{zz}^{GIAO}(\mathbf{r})$, $\sigma_{zz}^d(\mathbf{r}, \mathbf{R}_g = \mathbf{r})$ and $\sigma_{zz}^p(\mathbf{r})$ contour plots in Figures 1–4 look like accentuated versions of the respective $\sigma_{iso}^{GIAO}(\mathbf{r})$, $\sigma_{iso}^d(\mathbf{r}, \mathbf{R}_g = \mathbf{r})$ and $\sigma_{iso}^p(\mathbf{r})$ contour plots. In a planar molecule, if the z axis is perpendicular to the molecular plane, within the molecular plane $\sigma_{xz}(\mathbf{r}) = \sigma_{yz}(\mathbf{r}) = \sigma_{zx}(\mathbf{r}) = \sigma_{zy}(\mathbf{r}) = 0$, $\sigma_{zz}(\mathbf{r})$ and the sum $\sigma_{xx}(\mathbf{r}) + \sigma_{yy}(\mathbf{r})$ remain invariant with respect to the choices for the x and y axes, and the positional dependence of each of these shielding quantities can be studied on its own. The analyses of the $\sigma_{zz}^{GIAO}(\mathbf{r})$, $\sigma_{zz}^d(\mathbf{r}, \mathbf{R}_g = \mathbf{r})$ and $\sigma_{zz}^p(\mathbf{r})$ contour plots lead to very much the same conclusions as those of the respective $\sigma_{iso}^{GIAO}(\mathbf{r})$, $\sigma_{iso}^d(\mathbf{r}, \mathbf{R}_g = \mathbf{r})$ and $\sigma_{iso}^p(\mathbf{r})$ contour plots but the wider ranges of variation of $\sigma_{zz}^{GIAO}(\mathbf{r})$, $\sigma_{zz}^d(\mathbf{r}, \mathbf{R}_g = \mathbf{r})$ and $\sigma_{zz}^p(\mathbf{r})$ may provide interpretational advantages when investigating the aromaticity of other planar cyclic conjugated molecules. The $\sigma_{zz}^{GIAO}(\mathbf{r})$ contour plots in the molecular planes of benzene and square cyclobutadiene (Figures 1 and 2) are very similar to the contour plots of the z -component of the induced magnetic field, $B_z^{ind}(\mathbf{r})$, in the molecular planes of benzene and rectangular (D_{2h}) cyclobutadiene calculated using closed-shell density functional theory (DFT).^[30–32] The induced magnetic field is defined as

$B^{ind}(\mathbf{r}) = -\sigma(\mathbf{r})\mathbf{B}$ where \mathbf{B} is an external static spatially uniform magnetic field around the molecule. For a planar molecule with a z axis perpendicular to the molecular plane $B_z^{ind}(\mathbf{r})$ is proportional to $\sigma_{zz}(\mathbf{r})$, $B_z^{ind}(\mathbf{r}) = -\sigma_{zz}(\mathbf{r})B_z$. It should be noted that rectangular (D_{2h}) C_4H_4 is considerably less antiaromatic than square (D_{4h}) C_4H_4 ^[19,33–34] but closed-shell methods significantly overestimate its antiaromaticity.^[19]

The $\sigma_{iso}^{GIAO}(\mathbf{r})$, $\sigma_{iso}^d(\mathbf{r}, \mathbf{R}_g = \mathbf{r})$, $\sigma_{iso}^p(\mathbf{r})$, $\sigma_{zz}^{GIAO}(\mathbf{r})$, $\sigma_{zz}^d(\mathbf{r}, \mathbf{R}_g = \mathbf{r})$ and $\sigma_{zz}^p(\mathbf{r})$ contour plots in planes parallel to and 1 Å above the molecular planes of C_6H_6 and C_4H_4 (Figures 3 and 4) are simpler and easier to interpret than the respective contour plots in the molecular planes (Figures 1 and 2). Similarly to NICS(1) and NICS(1)_{zz}, these plots show mainly shielding effects associated with the π electrons. The $\sigma_{iso}^{GIAO}(\mathbf{r})$ contour plots in planes parallel to and 1 Å above the molecular planes of polycyclic aromatic hydrocarbons (PAHs) have been shown^[14,35] to capture the essence of the popular Clar aromatic sextets with high accuracy, providing visual and yet quantitative vindication of Clar's ideas. It should be noted that, at positions in the plane parallel to and 1 Å above the molecular plane different from that used to calculate NICS(1), at least two of the components $\sigma_{xz}(\mathbf{r})$, $\sigma_{yz}(\mathbf{r})$, $\sigma_{zx}(\mathbf{r})$ and $\sigma_{zy}(\mathbf{r})$ are non-zero which makes the use of the zz components of the shielding tensor and its diamagnetic and paramagnetic contributions calculated in that plane less well-justified than the use of the respective quantities calculated in the molecular plane.

While it is possible to choose between the $\sigma_{iso}(\mathbf{r})$ and $\sigma_{zz}(\mathbf{r})$ contour plots when describing planar conjugated molecules, for nonplanar molecules of this type it becomes necessary to use $\sigma_{iso}(\mathbf{r})$ isosurfaces. Examples are provided by the off-nucleus magnetic shielding studies of the aromaticities of norcorrole^[33] and corannulene.^[36]

As it was mentioned in the Introduction, the current CASSCF-GIAO calculations include nondynamic electron correlation effects only. However, the addition of dynamic electron correlation effects, for example, through a CASPT2-GIAO construction (second-order perturbation theory on top of a CASSCF-GIAO reference), if and when the required theory and codes become available, is unlikely to introduce other than relatively minor changes in the results of the current investigation. As it was shown in Ref. [19], the NICS(0), NICS(0)_{zz}, NICS(1) and NICS(1)_{zz} values for benzene calculated using the HF-GIAO method (which does not include electron correlation effects), the MP2-GIAO method (which includes dynamic correlation effects) and the CASSCF(6,6)-GIAO method are reasonably similar. It is not appropriate to calculate “broken-symmetry” HF-GIAO and MP2-GIAO NICS values for square cyclobutadiene, as its electronic ground state is an open-shell singlet, but both of these methods were found to produce similar NICS(0), NICS(0)_{zz}, NICS(1) and NICS(1)_{zz} values and to significantly overestimate the antiaromaticity of rectangular (D_{2h}) cyclobutadiene, in comparison to CASSCF(4,4)-GIAO – this is an indication that the off-nucleus shielding in cyclobutadiene is much more influenced by nondynamic than it is by dynamic electron correlation effects.

Conclusions

It has become a rule of the thumb in chemistry, similarly to Hückel's $4n + 2/4n$ π electron counts, to associate aromaticity with negative NICS values and antiaromaticity with positive NICS values. The analysis of the diamagnetic and paramagnetic contributions to a range of NICS indices for the classical examples of aromatic and antiaromatic molecules, benzene and square cyclobutadiene, shows that each of these contributions is of the same sign in the two molecules, and that the opposite signs of the overall NICS values are due to a change in the balance between the two contributions. According to the current results, the positive diamagnetic contributions to NICS(0), NICS(0)_{zz}, NICS(1) and NICS(1)_{zz}, which depend on the electron density, decrease significantly in magnitude on passing from benzene to cyclobutadiene and this decrease turns out to be just as important as the parallel increase in the magnitudes of the respective negative paramagnetic contributions which depend on perturbability of the wavefunction by an external magnetic field. This is an indication that the differences between the NICS values for antiaromatic and aromatic molecules cannot be attributed to differences in the ease of access to excited states only; differences in the electron density, a ground state property associated with the overall bonding picture in a molecule, also play an important role.

Qualitatively, when studied as functions of position in molecular space, the diamagnetic contributions to the isotropic shielding and to the zz component of the shielding tensor are shown to behave in a similar fashion in benzene and square cyclobutadiene, shielding the interior of the ring and its surroundings; the paramagnetic contributions to these quantities also behave similarly, but in the opposite manner, deshielding the interior of the ring and its surroundings. Both types of contribution are observed to be much larger inside the ring, hence the higher sensitivity of the various types of NICS as aromaticity probes in comparison to the shieldings or chemical shifts of exterior protons. Similar differences can be expected in aromatic and antiaromatic rings with both interior and exterior protons, for example, [18]annulene.^[37] The substantial differences between the variations of the off-nucleus isotropic shielding and of the zz component of the off-nucleus shielding tensor around benzene and square cyclobutadiene are shown to follow, in very much the same manner as the differences between the respective NICS values, from changes in the balance between the diamagnetic and paramagnetic contributions to these quantities.

Conflict of Interest

The authors declare no conflict of interest.

Data Availability Statement

The data that support the findings of this study are available in the supplementary material of this article.

Keywords: Aromaticity · antiaromaticity · nucleus-independent chemical shift · diamagnetic contribution · paramagnetic contribution

- [1] P. v. R. Schleyer, C. Maerker, A. Dransfeld, H. Jiao, N. J. R. v. E. Hommes, *J. Am. Chem. Soc.* **1996**, *118*, 6317–6318.
- [2] M. Solà, A. I. Boldyrev, M. K. Cyranski, T. M. Krygowski, G. Merino, *Aromaticity and Antiaromaticity: Basics and Applications*, John Wiley & Sons, Hoboken, **2023**.
- [3] P. v. R. Schleyer, H. Jiao, N. J. R. v. E. Hommes, V. G. Malkin, O. Malkina, *J. Am. Chem. Soc.* **1997**, *119*, 12669–12670.
- [4] P. v. R. Schleyer, M. Manoharan, Z. X. Wang, B. Kiran, H. Jiao, R. Puchta, N. J. R. v. E. Hommes, *Org. Lett.* **2001**, *3*, 2465–2468.
- [5] I. Cernusak, P. W. Fowler, E. Steiner, *Mol. Phys.* **2000**, *98*, 945–953.
- [6] E. Steiner, P. W. Fowler, L. W. Jenneskens, *Angew. Chem. Int. Ed.* **2001**, *40*, 362–366; *Angew. Chem.* **2001**, *113*, 375–379.
- [7] H. Fallah-Bagher-Shaidaei, C. S. Wannere, C. Corminboeuf, R. Puchta, P. v. R. Schleyer, *Org. Lett.* **2006**, *8*, 863–866.
- [8] C. Foroutan-Nejad, S. Shahbazian, F. Feixas, P. Rashidi-Ranjbar, M. Solà, *J. Comput. Chem.* **2011**, *32*, 2422–2431.
- [9] C. Foroutan-Nejad, *Theor. Chem. Acc.* **2015**, *134*, 8.
- [10] S. Fias, P. W. Fowler, J. L. Delgado, U. Hahn, P. Bultinck, *Chem. Eur. J.* **2008**, *14*, 3093–3099.
- [11] S. van Damme, G. Acke, R. W. A. Havenith, P. Bultinck, *Phys. Chem. Chem. Phys.* **2016**, *18*, 11746–11755.
- [12] P. B. Karadakov, K. E. Horner, *J. Phys. Chem. A* **2013**, *117*, 518–523.
- [13] P. B. Karadakov, P. Hearnshaw, K. E. Horner, *J. Org. Chem.* **2016**, *81*, 11346–11352.
- [14] P. B. Karadakov, B. VanVeller, *Chem. Commun.* **2021**, *57*, 9504–9513.
- [15] P. B. Karadakov, N. Preston, *Phys. Chem. Chem. Phys.* **2021**, *23*, 24750–24756.
- [16] W. H. Flygare, *Chem. Rev.* **1974**, *74*, 653–687.
- [17] J. Gauss, K. Ruud, T. Helgaker, *J. Chem. Phys.* **1996**, *105*, 2804–2812.
- [18] D. Sundholm, J. Gauss, A. Schäfer, *J. Chem. Phys.* **1996**, *105*, 11051–11059.
- [19] P. B. Karadakov, *J. Phys. Chem. A* **2008**, *112*, 7303–7309.
- [20] W. H. Flygare, J. Goodisman, *J. Chem. Phys.* **1968**, *49*, 3122–3125.
- [21] G. Malli, C. Froese, *Int. J. Quantum Chem.* **1967**, *1*, 95–98.
- [22] P. Seal, S. Chakrabarti, *J. Phys. Chem. A* **2007**, *111*, 9988–9994.
- [23] R. B. Ditchfield, *Mol. Phys.* **1974**, *27*, 789–807.
- [24] S. Radenković, S. Đorđević, *Phys. Chem. Chem. Phys.* **2021**, *23*, 11240–11250.
- [25] N. C. Baird, *J. Am. Chem. Soc.* **1972**, *94*, 4941–4948.
- [26] P. B. Karadakov, *J. Phys. Chem. A* **2008**, *112*, 12707–12713.
- [27] M. Rosenberg, C. Dahlstrand, K. Kilså, H. Ottosson, *Chem. Rev.* **2014**, *114*, 5379–5425.
- [28] R. Papadakis, H. Ottosson, *Chem. Soc. Rev.* **2015**, *44*, 6472–6493.
- [29] P. B. Karadakov, M. Di, D. L. Cooper, *J. Phys. Chem. A* **2020**, *124*, 9611–9616.
- [30] G. Merino, T. Heine, G. Seifert, *Chem. Eur. J.* **2004**, *10*, 4367–4371.
- [31] T. Heine, R. Islas, G. Merino, *J. Comput. Chem.* **2007**, *28*, 302–309.
- [32] R. Islas, T. Heine, G. Merino, *Acc. Chem. Res.* **2012**, *45*, 215–228.
- [33] P. B. Karadakov, *Org. Lett.* **2020**, *22*, 8676–8680.
- [34] S. Pathak, R. Bast, K. Ruud, *J. Chem. Theory Comput.* **2013**, *9*, 2189–2198.
- [35] B. J. Lampkin, P. B. Karadakov, B. VanVeller, *Angew. Chem. Int. Ed.* **2020**, *59*, 19275–19281; *Angew. Chem.* **2020**, *132*, 19437–19443.
- [36] P. B. Karadakov, *Chemistry* **2021**, *3*, 861–872.
- [37] F. Sondheimer, *Acc. Chem. Res.* **1972**, *5*, 81–91.

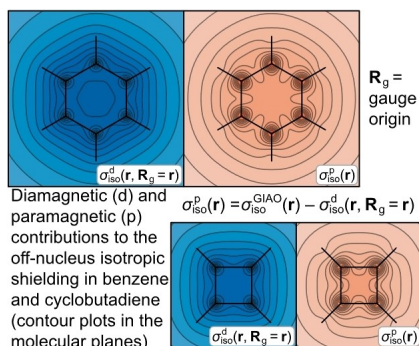
Manuscript received: January 17, 2023

Revised manuscript received: February 15, 2023

Accepted manuscript online: February 22, 2023

Version of record online: ■■■

Analysis of the diamagnetic and paramagnetic contributions to off-nucleus shielding in benzene and cyclobutadiene shows that the different off-nucleus shielding pictures and nucleus-independent chemical shift (NICS) values for antiaromatic and antiaromatic molecules cannot be attributed to differences in the ease of access to excited states only; differences in the electron density, which determines the overall bonding pattern, also play an important role.



Prof. Dr. P. B. Karadakov*

1 – 8

How Different are the Diamagnetic and Paramagnetic Contributions to Off-Nucleus Shielding in Aromatic and Antiaromatic Rings?

